RNA splicing variants of the novel long non-coding RNA, CyKILR, possess divergent biological functions in non-small cell lung cancer.

Xiujie Xie[1]*, H. Patrick Macknight[1], Amy L. Lu[1], and Charles E. Chalfant[1-4]*#

Affiliations:

[1]Department of Medicine, Division of Hematology & Oncology, University of Virginia, Charlottesville, VA, 22903

[2]Department of Cell Biology, University of Virginia, Charlottesville, VA, 22903

[3]Program in Cancer Biology, University of Virginia NCI Comprehensive Cancer Center, Charlottesville, VA, 22903

[4]Research Service, Richmond Veterans Administration Medical Center, Richmond VA, 23298

*Contributed equally as senior authors

#To whom correspondence should be addressed: Charles E. Chalfant, Professor, Department of Medicine, Division of Hematology & Oncology, P.O. Box 801398, University of Virginia-School of Medicine, Charlottesville, VA, 22903, email: cechalfant@virginia.edu or charles.chalfant@va.gov

Running Title: Divergent biological functions of CyKILR splice variants in NSCLCs

Key words: Long noncoding RNAs, RNA splicing, non-small cell lung cancers, Antisense Oligonucleotides, CDKN2A, LKB1, STK11

ABSTRACT

The CDKN2A gene, responsible for encoding the tumor suppressors p16(INK4A) and p14(ARF), is frequently inactivated in non-small cell lung cancer (NSCLC). In this study, an uncharacterized long non-coding RNA (lncRNA) (ENSG00000267053) on chromosome 19p13.12 was found to be overexpressed in NSCLC cells with an active CDKN2A gene. This lncRNA, named **Cy**clin-Dependent **K**inase **I**nhibitor 2A-regulated **l**nc**R**NA (CyKILR), also correlated with the STK11 gene-coded tumor suppressor Liver kinase B1 (LKB1). CyKILR displayed two splice variants, CyKILRa (with exon 3) and CyKILRb (without exon 3), which are synergistically regulated by CDKN2A and STK11 as knockdown of both tumor suppressor genes led to a significant loss of exon 3 inclusion in mature CyKILR RNA. CyKILRa localized to the nucleus, and its downregulation using antisense RNA oligonucleotides enhanced cellular proliferation, migration, clonogenic survival, and tumor incidence. In contrast, CyKILRb localized to the cytoplasm, and downregulation of CyKILRb using siRNA reduced cell proliferation, migration, clonogenic survival, and tumor incidence. Transcriptomics analyses revealed enhancement of apoptotic pathways with concomitant suppression of key cell cycle pathways by CyKILRa demonstrating its tumor-suppressive role, while CyKILRb inhibited tumor suppressor microRNAs, indicating an oncogenic nature. These findings elucidate the intricate roles of lncRNAs in cell signaling and tumorigenesis.

INTRODUCTION

Non-small cell lung cancers (NSCLCs) encompass a diverse group of lung malignancies, accounting for approximately 85% of all lung cancer cases.[1] Despite significant progress in diagnosis and treatment, NSCLCs remain a leading cause of cancer-related deaths worldwide.[2] The intricate molecular landscape of NSCLCs, characterized by complex tumor microenvironments and diverse genetic alterations, presents considerable challenges in understanding their pathogenesis and developing effective therapeutic strategies. In regard to genetic alterations, the cyclin-dependent kinase inhibitor 2A (CDKN2A) gene encodes the tumor suppressors, p16(INK4A) and p14(ARF), and is found inactivated or deleted in NSCLC at a high percentage. p14ARF is an alternate reading frame protein product of the CDKN2A locus, and p14ARF is induced in response to elevated mitogenic stimulation, such as aberrant growth signaling from the *MYC* and *RAS* genes. It accumulates mainly in the nucleolus where it forms stable complexes with NPM or Mdm2. p16INK4a (also known as cyclin-dependent kinase inhibitor 2A, multiple tumor suppressor 1, and numerous other synonyms) is a protein that suppresses cell division by slowing the progression of the cell cycle from the G1 phase to the S phase, thereby acting as a tumor suppressor. Loss of either p14ARF or p16INK4a has dramatic effects on the landscape of gene expression and RNA transcription increasing the susceptibility of cells to undergo oncogenic transformation.

Effects on gene expression can also include long noncoding RNAs (lncRNAs), which were for many years dismissed as "transcriptional noise". In recent years, lncRNAs have gained significant attention due to their potential roles in various diseases including cancer.[3-6] LncRNAs are RNA transcripts with lengths exceeding 200 nucleotides, and differ from protein-coding genes in not encoding for functional proteins. Instead, they exert their biological effects through diverse molecular mechanisms. With unique secondary and tertiary structures, lncRNAs can regulate gene expression through processes like chromatin modification, RNA splicing, and mRNA transcriptional and post-transcriptional regulation via RNA-DNA, RNA-microRNA, or RNA-Protein interactions.[7-11] In cancer biology, dysregulation and aberrant expression of lncRNAs have been linked to tumor initiation, progression, and therapeutic responses.[12] Distinct lncRNA expression patterns have been observed in various cancer types, including lung, breast, prostate, and

colorectal cancers, among others.[13-17] Furthermore, accumulating evidence suggests that lncRNAs can act as oncogenes or tumor suppressors exerting both pro-tumorigenic or anti-tumorigenic effects.[18, 19]

Like protein-coding genes, lncRNA genes consist of introns and exons that undergo alternative splicing. LncRNA splicing plays a pivotal role in generating transcriptomic diversity and expanding the functional repertoire of lncRNAs. Alternative splicing events give rise to distinct isoforms of lncRNA, which can differ in their sequences, structures, and subcellular localization. These splice variants possess the remarkable capacity to differentially modulate gene expression and cellular function in a context-dependent manner.[20-22] Although lncRNAs and their splicing variants have emerged as crucial players in the intricate landscape of cellular gene regulation,[23] identifying lncRNAs and their various splice variants remains challenging despite advancements in high-throughput sequencing technologies and bioinformatics approaches. Notably, one identified lncRNA, Neat1, undergoes alternative splicing regulated by RBM10, resulting in two splice variants, Neat1-1 and Neat1-2, which play distinct roles in the invasion and metastasis of NSCLCs.[24] Another reported lncRNA has multiple splice variants, SOX2OT (4 & 7), which have oncogenic roles in NSCLCs.[25] Thus, the alternative splicing of lncRNAs is becoming appreciated for their distinct and novel roles in NSCLC and cancer, but are significantly understudied.

In this study, we have made the exciting discovery of a novel lncRNA (ENSG00000267053) located on the forward strand of chromosome 19p13.12 that exhibits multiple splice variants. This lncRNA, termed **Cy**clin-Dependent **K**inase **I**nhibitor 2A-regulated **l**nc**R**NA (CyKILR), is almost exclusively present in NSCLC cells with both an active and wild-type *CDKN2A* and *STK11* gene. Based on the presence of exon 3, the CyKILR splice variants are classified into two distinct groups, CyKILRa (exon 3 included) and CyKILRb (exon 3 excluded). Mechanistic studies show that CyKILRa predominantly localizes in the nucleus and demonstrates a tumor-suppressive function. In contrast, CyKILRb localizes to the cytoplasm and exhibits prosurvival functions. The balance between the two groups of CyKILR RNA splicing variants is dynamically regulated by gene products of both the *CDKN2A* and *STK11* genes, thereby finely tuning cellular homeostasis in these NSCLC cell lines. Our findings shed light on the potential diagnostic, prognostic, and therapeutic implications of targeting lncRNAs and their specific splicing variants in NSCLCs opening new avenues for precision medicine approaches. Indeed, this study also unravels the

87 intricate regulatory networks orchestrated by lncRNAs and their splice variants offering an exciting
88 opportunity to decipher their complex roles in cancer biology.

89

90 **MATERIALS AND METHODS**

91 ***Cell lines and materials***

92 NCI-358, NCI-H522, NCI-H2009, NCI-H810, NCI-H460, A549, NCI-H838, NCI-H1734, NCI-H1648,
93 NCI-H2030, NCI-H1299, NCI-H1792, and human bronchial epithelial cells (HBECs) were purchased from
94 ATCC. RNA Subcellular Isolation Kit was from Active Motif (25501). SuperScript™ IV VILO™ Master
95 Mix with ezDNase™ Enzyme (11766050), TaqMan™ Universal PCR Master Mix (4324018), Opti-
96 MEM™ I Reduced Serum Medium (31985062), Lipofectamine™ RNAiMAX Transfection Reagent
97 (13778150), and Pierce Fast Western Blot Kit (35050) were from Thermo Fisher Scientific. Cell Titer-Glo
98 2.0 Assay Kit was purchased from Promega (G9242). The mycoplasma contamination detection kit was
99 purchased from InvivoGen (rep-mys-50).

100 ***Cell culture***

101 All cells were cultured following the procedures described previously and were utilized within 6 months or
102 -twenty passages, whichever came first, from the time of receipt and thawing. [26] Throughout the entire study,
103 cell lines were subjected to Mycoplasma testing every two months using a Mycoplasma contamination
104 detection kit. Parental cell lines were authenticated by STR (short tandem repeat) profiling.

105 ***Transcriptomics and Splicomic analyses***

106 *Short-Read:* RNA sequencing was conducted using 150 bp paired-end reads, aiming for a depth of
107 approximately 90 million reads. Sequencing reads were aligned to the GRCh38.p14 reference genome using
108 STAR software (v2.7.10b), and post-alignment, BAM files were filtered and indexed with Samtools
109 (v1.16.1) to remove low-quality reads.[27, 28] For differential gene expression analysis, the R package DESeq2
110 was utilized on previously described RNAseq data processed with Salmon 1.10.0.[29, 30] Additional R
111 packages employed included tximport for importing data, biomaRt for genomic annotation, tidyverse for
112 statistical analyses, RColorBrewer for color palettes, and org.Hs.eg.db for gene annotations.[31-33] Isoform

113 detection and quantification was performed using the previously described Salmon processed RNAseq data.
114 Transcript IDs for genes of interest were identified from the GENCODE v45 comprehensive annotation .gtf
115 file. These IDs facilitated parsing of Salmon .sf files to obtain TPM values for each transcript, which
116 informed our transcript abundance calculations. Finally, TPM values for selected transcripts were visualized
117 using the tidyverse package in R version 4.3.3.[31] Differential alternative splicing analysis was performed
118 on these filtered BAM files using rMATS turbo (v4.1.2).[34] Subsequently, R programming language was
119 utilized to filter and generate a list of splicing targets from the data produced by rMATS.

120 ***RNA extraction and Quantitative RT-PCR***

121 Total RNA and subcellular RNA were isolated from cultured cells using the RNA Subcellular Isolation Kit
122 from Active Motif (25501) following the manufacturer's instructions. RNA quantification was performed
123 using a NanoDrop NP-1000 spectrometer, and RNA (2 µg) was used for the first-strand cDNA synthesis
124 using SuperScript™ IV VILO™ Master Mix with ezDNase™ Enzyme. Subsequently, qRT-PCR was
125 conducted as done on a Quant Studio 5 instrument (Applied Biosystems, Carlsbad, CA, USA). [35-41] The
126 housekeeping gene GAPDH was utilized for normalization using the ΔΔCt method. The specific primers
127 and probes used in the study are listed in **Table S1**. A customized quantitative primer and probe strategy
128 for the detection of CyKILRa and CyKILRb variants was also employed. For CyKILRa Exon 3 inclusion
129 variants, we designed primers and probes specifically targeting Exon 3, as all CyKILRa variants in this
130 group contain Exon 3. In contrast, for CyKILRb Exon 3 exclusion variants, which lack Exons 2-4, the
131 forward primer aligns with Exon 1, the reverse primer is complementary to Exon 5, and a probe spans the
132 Exon 1 to Exon 5 junction.

133 ***Multiplex RT-PCR***

134 A reaction mixture was prepared by combining cDNA (25 ng) with both sets of primers at a final
135 concentration of 0.1 µM. To achieve a total volume of 50 µl, the cDNA-primer mixture was mixed with 2X
136 master mix and water. The PCR was performed using the hot-start method, with an annealing temperature
137 of 58°C for 26 cycles. The specific primers used in the study are listed in **Table S1**.

138 ***RNAi and ASOs Transfection***

139 Cells were plated in a full medium without antibiotics the day before transfection, ensuring they reached
140 50% confluency at the time of transfection. To dilute siRNA or ASOs, Opti-MEM® I Reduced Serum
141 Medium was used. For siRNA transfection, Lipofectamine RNAiMAX was employed as done,[42-46] while
142 Lipofectamine 3000 was used for ASOs transfection. The final concentration of both siRNA and ASOs in
143 the cell culture medium was 20nM. The sequences of siRNAs and ASOs are listed in **Table S1**. ASO was
144 customized 2′-*O*-methyl locked DNA chimera with phosphorothioate bonds backbone. siRNA was
145 customized 19-22 basepair duplex RNA with 3' UU overhangs.

146 ***Proliferation analysis***

147 To investigate cell proliferation, the Cell Titer-Glo Luminescent Cell Viability kit was utilized following
148 the manufacturer's instructions. Cells were initially seeded in 96-well plates at a density of 2000 cells per
149 well in RPMI1640 supplemented with 10% FBS. After treatment with ASO or siRNA for 48 hours, the
150 plates were carefully decanted and refilled with 50 µl of Cell Titer-Glo reagent and 50 µl of PBS per well.
151 The plates were then incubated for 10 minutes at room temperature in the dark. Subsequently, the
152 luminescence readings were taken using the Gene5 Multi-Mode Microplate Reader (Molecular Devices,
153 Sunnyvale, CA) with a 250 ms integration.

154 ***Cell survival assays***

155 After ASO or siRNA treatment, cells were harvested and re-suspended in complete growth media.
156 Subsequently, the cells (2-4 x10^2) were seeded onto six-well plates and allowed to grow until visible
157 colonies formed as done,[35-39, 47-49] which typically occurred within 7-21 days depending on the cell line.
158 Once the colonies became visible, they were fixed with cold methanol, stained with 0.25% crystal violet in
159 25% methanol, washed, and then left to air-dry.

160 ***Cell Migration***

161 The scratch migration assay was conducted following the procedure previously described.[50-53] Briefly,
162 ASOs- or siRNA-treated cells were cultured in 6-well plates with RPMI 1640 medium containing 10% FBS
163 until they reached 90% confluency. An ~1 mm cell-free gap was created using a sterile pipette tip. After
164 washing away dislodged cells with PBS, the plates were refilled with fresh medium and incubated for 24

hours before capturing images. Cell migration was quantified using Image J software, analyzing the change in the cell-free area at 0 hours and 24 hours.

Western immunoblotting

Cells were lysed in RIPA buffer containing Halt™ Protease and Phosphatase Inhibitor Cocktail (Thermo Fisher Scientific, 78440). For protein concentration determination, the Pierce BCA Protein Assay kit (Thermo Fisher Scientific, 23227) was used.[40, 54-56] Whole-cell lysates were mixed with Laemmli loading buffer, boiled, separated by 4-20% SDS–PAGE, and transferred to a PVDF membrane as done.[54, 56-61] Subsequently, immunoblot analyses were performed using specific antibodies (see source companies, catalog numbers, and dilution ratios listed in **Table S2**). The specific protein bands were visualized by using Western Blotting Kit (Pierce, 35050).

Mouse tumor xenograft models

Five-week-old female NOD-SCID mice were subcutaneously injected with H1792 or H2009 cells ($1x10^6$) mixed in Matrigel solution (50%) into the hind flanks as previously done by us.[35-37, 47, 48] Tumor size was measured 2 to 3 times per week using a vernier caliper. Once the tumors reached approximately 100 mm^3 in size, the mice were randomly assigned to either the scramble control or knockdown group. When the tumor size reached 1000 mm^3, the mice were euthanized, and the tumors were excised for weight measurement and histological analysis. Throughout the study, all animals were maintained according to the University of Virginia (protocol#4372-11-21) and Richmond VAMC (IRBnet ID#1654460-4) approved IACUC protocols.

Signaling Pathway Analyses

The sequencing data was filtered with SOAPnuke (v1.5.6) (removing reads containing sequencing adapter and low-quality base ratio), then the clean reads were stored in FASTQ format. [62] Differential expression gene (DEG) analysis was performed using the DESeq2 with Q value $\leqslant$ 0.05. [30] KEGG enrichment analysis of annotated different expression gene was performed by R Phyper (v120.0) based on Hypergeometric test. The significant levels of terms and pathways were corrected by Q value with a rigorous threshold (Q value $\leqslant$ 0.05).

191 ***Statistical analysis***

192 Graphing and statistics were performed using Prism GraphPad (Prism Software, San Diego, CA). The
193 following models were used for statistical analysis as described, unpaired t-test with Welch's correction
194 were used when only two experimental groups were being compared. Repeated measures ANOVA were
195 used when analyzing comparison groups that contained a dependent variable that was measured several
196 times over the course of the experiment. One-way ANOVA with Tukey's multiple comparisons test were
197 used when comparing three or more independent groups. Two-way ANOVA with Šídák's multiple
198 comparisons were used when an examination of how the combination of two independent variables affected
199 a dependent variable. All data reported as boxplot or mean (SD) where applicable; $p < 0.05$ was considered
200 statistically significant. All bioinformatic analyses were conducted using the R program.

201

202 **RESULTS**

203 **The association of the expression of a novel long non-coding RNA and CDKN2A/LKB1 status in**
204 **NSCLCs**

205 The *CDKN2A* gene is found inactivated or deleted in NSCLC at a high percentage, which also means that
206 a number of NSCLC tumors and cell lines have a wild-type (WT), active, and functional *CDKN2A* gene.
207 To examine if there are specific gene expression patterns between WT *CDKN2A* versus mutant/inactive
208 *CDKN2A* NSCLC cell lines, twelve NSCLC cell line with a differing *CDKN2A* status were compared (six
209 with WT *CDKN2A* (H838, H522, H2009, H1299, H1792, and H1734) and six with deleted/mutant
210 *CDKN2A* (H2030, H810, H460, A549, H838, and H1648)) using unbiased transcriptomics. A top "hit" for
211 a differential RNA linked to a WT *CDKN2A* gene was a novel, uncharacterized lncRNA
212 (ENSG00000267053) located on chromosome 19p13.12. Validation studies using qRT-PCR corroborated a
213 strong link between this **Cy**clin-Dependent **K**inase **I**nhibitor 2A-regulated **l**nc**R**NA (CyKILR) and the WT
214 *CDKN2A* gene, but a perfect correlation was not observed (**Fig.1A-C**). The DESeq2 and plot3 packages in
215 R studio were also utilized to generate both 3D principal component analysis (PCA) and correlation plots
216 of CDKN2A mRNA expression with CyKILR expression, but the PCA showed that the 12 NSCLC lines

217 did not exhibit strong clustering based solely on CDKN2A status/expression (**Fig.1D**). Examining
218 additional oncogenotypes to explain the inconsistency showed that the five NSCLC cell lines with high
219 CyKILR expression (H358, H522, H2009, H1299, H1792) also correlated with the expression of the tumor
220 suppressor, Liver kinase B1 (LKB1), a product of the *STK11* gene (**Fig.1E,F**). The protein levels of the
221 *CDKN2A* gene products, p14 ARF and p16 INK4A, as well as LKB1 were also examined to validate our
222 transcriptomic and qRT-PCR findings (**Fig.1G,H**), and the results were consistent with the mRNA
223 expression findings across the 12 cell lines although previously reported CDKN2A mutant cells lines
224 showed significant p14 or p16 expression (H2030 and H810). Importantly, our analyses revealed high
225 expression of CyKILR in only H358, H522, H2009, H1299, and H1792, which were cell lines positive for
226 both WT *CDKN2A* and *STK11* genes (**Fig.1G,H)**. These results demonstrate that CyKILR is almost
227 exclusively expressed in NSCLC cell lines with both active and WT *CDKN2A* and *STK11* genes.

228 **CyKILR classifies into two distinct isoform groups based on the alternative RNA splicing of Exon 3**

229 RNA sequencing data revealed the presence of multiple variants of CyKILR as depicted in **Figure 2A,B.**
230 To categorize these variants, we employed a classification based on the status of Exon 3. Those variants
231 containing Exon 3 were designated as CyKILRa, while those lacking Exon 3 were denoted as CyKILRb.
232 To evaluate their relative expression patterns, we conducted RT-PCR across a panel of 12 NSCLC lines. As
233 shown in **Figure 2C**, expression of the CyKILRa group was easily detected in H358, H522, H2009, H1299,
234 H1792, and H1648 cell lines. Moreover, a discernable level of expression was also observed in H2030,
235 H1734, and H810 cell lines. In contrast, H460, A549, and H838 showed minimal to negligible expression
236 of the CyKILRa group, the cell lines completely devoid of both CDKN2A and STK11 gene products by
237 Western immunoblotting (**Fig.1G**). Conversely, the cohort of CyKILRb displayed expression exclusively
238 within the H358, H522, H2009, H1299, and H1792 cell lines (**Fig.2C**), NSCLC cell lines with discernable
239 expression of both CDKN2A and STK11 gene products by Western immunoblotting (**Fig.1G**). To quantify
240 the expression level of CyKILRa and CyKILRb across the 12 NSCLC lines, we employed customized
241 quantitative primers and probes (**Fig.2D**). To target Exon 3 inclusion variants, the primers, and probes were
242 designed to be complementary to Exon 3 (**Fig.2D**). In contrast, for the identification of Exon-exclusive
243 variants, the forward primer corresponded to Exon 1, while the reverse primer aligned with Exon 5,

complemented by a probe spanning the junction of Exon 1 and Exon 5 (**Fig.2D**). Our results revealed that both CyKILRa and CyKILRb were predominantly expressed in H358, H522, H2009, H1299, and H1792 cell lines (**Fig.2D**), which are characterized by the presence of both active and WT *CDKN2A* and *STK11* genes (CyKILR expression in WT *CDKN2A*/WT *STK11* NSCLC lines verified by Western immunoblotting) vs other NSCLC cell lines, p = 0.000729 for n=4/cell line using One Way ANOVA). These data also demonstrate that CyKILRb has more distinct expression linked to these tumor suppressing genes.

CyKILRa and CyKILRb RNA splicing variants display differential cellular localization

Unlike mRNA, lncRNA is frequently detected in both the cytoplasm and nucleus. Research in the area suggests that an "AGCCC" motif plays a crucial role in the nuclear localization of numerous lncRNAs.[63] Following a sequence analysis, the specific presence of the "AGCCC" motif in Exon 3 of CyKILR was identified (**Fig.3A**). This discovery prompted us to investigate the localization patterns of the two distinct CyKILR groups by isolating total RNA from both the nucleus and cytoplasm as well as from whole cells. Subsequent multiplex and quantitative RT-PCR analyses highlighted a prevalent nuclear distribution for the variants containing Exon 3 (CyKILRa) in stark contrast a predominant cytoplasmic localization observed for the variants lacking Exon 3 (CyKILRb) (**Fig.3B,C**). Indeed, quantitative RT-PCR analyses showed >80% of CyKILRa variants clearly situated within the nucleus, while a corresponding percentage of >80% of CyKILRb variants consistently resided in the cytoplasm (**Fig.3C**). These data demonstrate that the presence or absence of exon 3 in the mature CyKILR transcript regulates the cellular localization of this lncRNA.

CDKN2A and LKB1 regulate CyKILR exon 3 exclusion

Our data showing a strong correlation between WT, active *CDKN2A* and *STK11* genes with CyKILR expression suggested that the gene products of these two tumor suppressors cooperated to “drive” CyKILR expression. Surprisingly, downregulation of mRNAs stemming from the CDKN2A and STK11 genes, individually or concomitantly, by siRNA (**Fig.4A**) did not yield consistent or conclusive effect on the total CyKILR RNA levels in NSCLC lines although significant reduction in CyKILR expression was observed in non-cancerous HBEC-3KT cells (**Fig.4A,B**). In additional mechanistic studies, the RNA levels of the two splice variant groups of CyKILR (CyKILRa and CyKILRb) were examined individually, and whereas,

270 individual downregulation of either CDKN2A or STK11 mRNAs by siRNA did not yield significant
271 changes in the ratio between the two splice variant groups, the co-downregulation of the mRNA products
272 of these two tumor suppressors led to a dramatic increase in the ratio of CyKILRb/CyKILRa variants
273 compared to control siRNA (**Fig.4C**). These data demonstrate that LKB1 and CDKN2A gene products act
274 to induce the inclusion of exon 3 into CyKILR RNA, which will enhance the expression of nuclear
275 CyKILRa.

276

277 The above findings inferred that induction of exon 3 inclusion into the mature CyKILR RNA transcript was
278 biologically pertinent in relation to functional *CDKN2A* and *STK1*1 genes. To investigate whether
279 suppression of CyKILRb expression affected biological phenotypes suppressed by the CDKN2A and
280 STK11 gene products, proliferation was assessed when these tumor suppressors were again co-
281 downregulated by siRNA. Downregulation of both CDKN2A and STK11-derived mRNAs induced a
282 significant increase in cell proliferation (**Fig.4D**). The simultaneous downregulation of CyKILRb
283 attenuated the increased proliferation observed following CDKN2A and LKB1 co-silencing as compared
284 to control siRNA cells (**Fig.4D**). These data show that suppression of CyKILRb expression via inclusion of
285 exon 3 is an important mechanism by which LKB1 and CDKN2A subdue cell proliferation.

286 **Nuclear CyKILRa and cytoplasmic CyKILRb have opposing functions *in vitro* and *in vivo***

287 Based on our data suggesting that CyKILR has biological functions linked to cancer cell phenotypes (e.g.,
288 cell proliferation), the role of the two specific CyKILR isoform groups was examined for effects on cell
289 proliferation, cell survival, and cell migration. First, the functional role of nuclear-localized CyKILR
290 variants (CyKILRa) was assessed, which required the utilization of DNA/RNA chimeric antisense
291 oligonucleotides (ASOs) to silence nuclear CyKILRa as siRNA has been shown ineffective for these nuclear
292 forms of RNA[64]. The silencing efficacy of our ASOs exceeded 50% across all four tested cell lines (**Fig.5A**).
293 Downregulation of CyKILRa resulted in significant enhancement of cell proliferation (**Fig.5B**), and a >two-
294 fold acceleration in cell migration (**Fig.5C**). Furthermore, cell survival as assessed by clonogenic colony
295 plate assay was significantly increased in these cell lines by downregulation of CyKILRa (**Fig.5D**). In

296 addition, downregulation of CyKILRa had a significant and profound effect on tumor formation for both
297 H2009 and H1792. Specifically, downregulation of CyKILRa with ASOs induced significant tumor growth
298 and formation in both cell lines after four weeks, a time point when tumors were not appreciably formed in
299 the control cell lines (**Fig.5E**). In stark contrast, downregulation of CyKILRb by siRNA (**Fig.6A**) resulted
300 in a significant reduction of cell proliferation (**Fig.6B**). Additionally, a significant decrease in both cell
301 migration and cell survival was observed (**Fig.6C,D**). Downregulation of CyKILRb by siRNA also induced
302 a significant reduction in tumor growth when control tumors were allowed to grow to 200 mm^3 in volume
303 (**Fig.6E**). In all replicates, downregulation of CyKLRa and b produced profound effects on tumor growth
304 over the experimental time course (**Supplemental Fig.1**). These data demonstrate that nuclear CyKILRa
305 has specific cellular functions and acts to suppress key dysregulated pro-survival phenotypes observed in
306 NSCLC cells. Furthermore, cytosolic CyKILRb has an opposing function acting as a pro-survival, pro-
307 tumorigenic, and pro-growth factor.

308 **CyKILRa and CyKILRb have opposing functions on cell signaling pathways**

309 Since modulation of CyKILR splice variants showed strong effects on tumor biology and cancer cell
310 phenotypes, the mechanistic underpinnings were explored. In this regard, downregulation of CyKILRa and
311 b followed by deep RNA sequencing and pathway analysis was undertaken. Downregulation of CyKILRa
312 by ASOs showed decreased expression of factors central in apoptosis induction (e.g., Bak1, CHOP, PUMA)
313 as well as significantly increased expression of factors known to drive the cell cycle, cell proliferation, and
314 cell growth (e.g., CDK1, CDK2, CHEK2) (**Fig.7A-C; Supplemental Figures 2,3**). Downregulation of
315 CyKILRb, on the other hand, led to induction of tumor suppressing miRNAs, hsa-miR-424-3p and has-
316 miR-503-p (**Fig.7D-F**). Treatment of H2009 and H1299 cells with mimics of these two miRNAs partially,
317 but significantly suppressed key cancer cell proliferation (**Fig.7G**). These data show that CyKILR splice
318 variants have roles in the modulation of key pathways linked to both tumor suppression and tumorigenesis.

319

320 **DISCUSSION**

321 In this study, we have discovered a novel long non-coding RNA (lncRNA), which we termed **Cy**clin-
322 Dependent **K**inase **I**nhibitor 2A-regulated **l**nc**R**NA (CyKILR) due to its expression being mainly confined
323 to NSCLC lines harboring a wild-type and active *CDKN2A* gene. Additional studies showed that an
324 oncogenotype consisting of both a WT *CDKN2A* and *STK11* gene correlated stronger with the expression
325 of CyKILR, and downregulation of the mRNA of either gene led to significant loss of CyKILR expression
326 in non-transformed human bronchial epithelial cells. The loss of CyKILR expression observed in NSCLC
327 cell lines lacking either a WT STK11 or CDKN2A gene correlated and corroborated this finding, which
328 strongly suggested that CyKILR has a possible tumor suppressor role linked to the cell signaling pathways
329 activated by the LKB1 and CDKN2A gene products. In support of this conclusion, downregulation of the
330 CyKILRa isoforms (exon 3 included) significantly enhanced cell survival, migration, and proliferation as
331 well as tumor growth. On the other hand, downregulation of CDKN2A and STK11 mRNAs in NSCLC cell
332 lines with both WT STK11 and CDKN2A genes surprisingly demonstrated minimal or no significant effect
333 on total CyKILR expression. Thus, depending on the cellular context and oncogenic landscape,
334 maintenance of CyKILR expression becomes independent of these genes. Shedding light on a plausible
335 adaptive mechanism was the additional characterization of CyKILR, which identified multiple RNA splice
336 variants including an exon 3 excluded isoform designated CyKILRb. In contrast to CyKILRa, this splice
337 variant class was pro-survival, and notably, the ratio of CyKILRb/a, was very low in non-cancerous, human
338 bronchial epithelial cells, when compared to the NSCLC cell lines that expressed CyKILR. We posit that
339 shifting from the CyKILRa isoform to the CyKILRb isoform through modulation of exon 3
340 inclusion/exclusion by alternative RNA splicing is required for transformed NSCLC cells to maintain cell
341 homeostasis in the presence of these key tumor suppressors. Indeed, downregulation of CyKILRb had
342 dramatic effects in reducing the survival and tumor growth of NSCLC cells with WT STK11 and CDKN2A
343 genes. Specific downregulation of CyKILRb also blocked any enhancement of cellular proliferation
344 observed when both of these genes were inactivated. Therefore, the CyKILRb splice variants of this
345 lncRNA are plausible proto-oncogenes, or more specifically, these data suggest that exclusion of exon 3
346 from CyKILR RNA removes a key nuclear lncRNA required for LKB1 and CDKN2A gene products to act
347 as efficient tumor suppressors.

348 The observation that the STK11 and CDKN2A gene products co-regulated the alternative RNA
349 splicing of CyKILR was a unexpected finding. Indeed, a tremendous 30-fold increase in the CyKILRb/a
350 RNA ratio in HBECs was observed when CDKN2A and STK11 mRNAs are downregulated. This is a 10-
351 fold higher response than the NSCLC cells examined in this study, which suggests that transformed cells
352 with an active and WT CDKN2A and STK11 gene also have active oncogenic pathways with opposing
353 function on downstream RNA splicing, which act to suppress exon 3 inclusion. How the products of these
354 tumor suppressor genes regulate the inclusion/exclusion of CyKILR exon 3 is unknown opening avenues
355 of unanswered questions in relation to their tumor suppressing functions and the regulation of alternative
356 RNA splicing. Dysregulated alternative RNA splicing is well established in cancer with RNA *trans*-factors
357 acting as proto-oncogenes,[65] but there is essentially nothing reported in the literature as to alternative RNA
358 splicing regulation downstream of the signaling pathways regulated by CDKN2A and STK11 gene products.
359 There are reported links to the CDKN2A gene product, p16, in regulating the association of the RNA
360 binding protein, AUF1 to CDKN1A mRNA in regard to RNA stability.[66] The expression of hnRNP B1, an
361 RNA splicing factor, was reported as inversely regulated in relation to p16 expression in lung cancer
362 tissue.[67]. CDKN2A gene products as well as LKB1 will repress activation of the AKT pathway, and thus,
363 when CDKN2A and LKB1 are downregulated, AKT activation will occur, which is known to have distinct
364 effects on RNA splicing.[36-38, 68] This signaling paradigm is logical as loss of both pathways may cooperate
365 to enhance the expression of specific AKT isoforms, modulate specific post-translational modifications
366 related to AKT activation, and alteration of cellular topology via PIP_3 production in specific organelles such
367 as the nuclear membrane or nucleus itself. As to the latter, it has been previously surmised and shown that
368 AKT can directly phosphorylate RNA *trans*-factors in the nucleus to modulate specific RNA splicing
369 events.[36-38] Thus, coordinated modulation/suppression of nuclear AKT signaling may be one plausible route
370 for loss of these tumor suppressors to cooperate in regulating specific alternative splicing events.
371 Additionally, our study has not examined the alternative RNA splicing in the NSCLC cells lacking
372 appreciable CyKILR expression. Thus, downregulation and suppression of total CyKILR expression may
373 occur via the induction of CyKILR RNA splice variants removed by nonsense mediate RNA decay[69], which
374 is an efficient mechanism to remove aberrant mRNA transcripts that may arise from alternative RNA

splicing. Future studies are required to determine how loss of the *STK11* and *CDKN2A* tumor suppressors leads to suppression of CyKILR expression in NSCLC.

The characterization on CyKILR RNA splice variants in this study led to the observation of distinct subcellular distributions for CyKILRa and b, which corresponded to their divergent functions. Indeed, lncRNAs serve as operational units/scaffolds, and their subcellular localization plays a pivotal role in governing their functions.[70] For example, a substantial number of lncRNAs primarily reside within the nucleus, where they perform diverse regulatory functions through a multitude of combinatorial mechanisms optimized for nuclear enrichment.[71-74] In our study, we found that CyKILRa has a distinct nuclear localization in contrast to the cytoplasmic predominant localization of CyKILRb. Through in silico analysis, a potential nuclear retention motif, "AGCCC," was identified with -8 (T or A) and -3 (G or C) relative to the first nucleotide of the pentamer in Exon 3 of CyKILR[63]. Thus, CyKILRa predominance in localizing to the nucleus in contrast to CyKILRb is logical as this sequence only resides in exon 3. As to how CyKILRa functions as a tumor suppressor, its nuclear localization may be key to exerting regulatory influence over cellular processes, possibly through interactions with epigenetic factors involved in histone modification complex scaffolding or recruitment as previously reported for other lncRNAs.[39] Additionally, nuclear lncRNAs often assume additional roles including the modulation of pre-mRNA processing and involvement in alternative splicing events.[40] Uncovering the specific regulatory mechanisms governing CyKILRa within the nucleus holds great promise for precision-targeted tumor therapy as our transcriptomics analyses show that AKT levels were significantly increased in two separated NSCLC cells lines when CyKILRa was downregulated by ASO, and this pathway is potent in both survival signaling, oncogenesis, and in modulating alternative RNA splicing. Indeed, systems level analyses of the transciptome showed the apoptosis genes were downregulated and other pathways linked to enhancing the cell cycle were increased, which our laboratory confirmed by qRT-PCR and Western immunoblotting. These data support the inference that CyKILRa acts as a nuclear scaffold for regulating gene expression, specifically suppression of cell cycle pathways while simultaneously maintaining the levels of factors allowing for apoptosis to occur upon oncogenic stress.

401 In contrast to CyKILRa, CyKILRb functions as a pro-tumorigenic factor, and like CyKILRa, it is
402 currently unknown as to how CyKILRb functions in this role. Emerging research also suggests that the
403 population of cytoplasmic lncRNAs may be more abundant than previously recognized.[75-77] Cytoplasmic
404 lncRNAs have been implicated as a microRNA sponge, sequestering microRNAs or regulating protein
405 stability.[41] When lncRNAs function as miRNA "sponges", these non-coding RNAs act as competing
406 endogenous RNAs (ceRNAs),[43] which are reported to play key roles in cancer disease states.[44] In this regard,
407 systems level analysis of CyKILRb downregulation in two NSCLC cell lines with WT *STK11* and *CDKN2A*
408 genes found a consistent increase in two reported, tumor suppressing miRNAs, hsa-miR-424-3p and has-
409 miR-503-p.[78, 79] Interestingly, there is no complementary sequence for these miRNAs in CyKILRb
410 suggesting that the regulation of these miRNAs by CYKILRb is not through a "sponge" mechanism.
411 Regardless, examining this novel link between CyKILRb and the expression of hsa-miR-424-3p and has-
412 miR-503-p is a future mechanistic avenue to explore.

413 In conclusion, our study characterizes a novel lncRNA with functional roles in NSCLC with a
414 specific oncogenotype. The association with CDKN2A and LKB1 status, the differential subcellular
415 localization, and the impact on cellular behavior and in vivo tumorigenicity suggest that CyKILR splice
416 variants are important players in NSCLC pathogenesis. Further research is needed to elucidate the precise
417 molecular mechanisms underlying the functions of the individual CyKILR variants and their expression.
418 Indeed, this intricate interplay between the two subcellular groups of CyKILR underscores the critical
419 importance of their relative ratios offering a precise means to finely tune cellular progression. Additionally,
420 exploration as to its potential as a therapeutic target in NSCLC and potentially other cancer types is
421 warranted as RNA-based therapies are now plausible.[80] Overall, this study provides a foundation for future
422 investigations into the diagnostic and therapeutic implications of targeting specific lncRNA splicing
423 variants in NSCLCs, and future exploration of lncRNAs like CyKILR offers a promising avenue for
424 precision medicine approaches in cancer therapy.

425

426 **Acknowledgements:** The contents of this manuscript do not represent the views of the Department of
427 Veterans Affairs or the United States Government.

Funding: This work was mainly supported by the Veteran's Administration (VA Merit Review, BX001792 (to CEC), VA Merit Review award, BX 006063 (C.E.C.), and a Senior Research Career Scientist Award, IK6BX004603 (to CEC)). This work was peripherally supported by way of research cores, methodology and technology development, and software development by the National Institutes of Health by way of P01 CA171983 (Project 1 to CEC), NIH/NCI Cancer Center Support Grant P30 CA044579, and the R01s AI139072 (to CEC), and DK126444 (to CEC). This work was also supported by funds from the Department of Medicine in the University of Virginia-School of Medicine in regard to software licensing and equipment purchases.

Author Contributions: XX – designing research studies, conducting experiments, acquiring data, analyzing data, and writing the manuscript. HPM – developing and analyzing short and long read deep RNA sequencing data, manuscript method writing, and figure composition. ALL – conducting experiments, acquiring data, and analyzing data. CEC – overall supervision, designing research studies, analyzing data, providing reagents and funding, editing manuscript, and writing the manuscript.

Conflict of Interest Statement: The authors declare that they have no conflicts of interest.

Data and Materials Availability: All RNAseq data are in the process of submission to NCBI Sequence Read Archive (SRA) database for public access (Submission number: sub14341995).

REFERENCES

1. Chen Z, Fillmore CM, Hammerman PS, Kim CF, Wong KK. Non-small-cell lung cancers: a heterogeneous set of diseases. Nat Rev Cancer. 2014;14: 535-546.
2. Global Burden of Disease Cancer C, Fitzmaurice C, Abate D, et al. Global, Regional, and National Cancer Incidence, Mortality, Years of Life Lost, Years Lived With Disability, and Disability-Adjusted Life-Years for 29 Cancer Groups, 1990 to 2017: A Systematic Analysis for the Global Burden of Disease Study. JAMA Oncol. 2019;5: 1749-1768.
3. Khan MR, Avino M, Wellinger RJ, Laurent B. Distinct regulatory functions and biological roles of lncRNA splice variants. Mol Ther Nucleic Acids. 2023;32: 127-143.
4. Olivero CE, Martinez-Terroba E, Zimmer J, et al. p53 Activates the Long Noncoding RNA Pvt1b to Inhibit Myc and Suppress Tumorigenesis. Mol Cell. 2020;77: 761-774 e768.
5. Yuan JH, Liu XN, Wang TT, et al. The MBNL3 splicing factor promotes hepatocellular carcinoma by increasing PXN expression through the alternative splicing of lncRNA-PXN-AS1. Nat Cell Biol. 2017;19: 820-832.
6. Jiang MC, Ni JJ, Cui WY, Wang BY, Zhuo W. Emerging roles of lncRNA in cancer and therapeutic opportunities. Am J Cancer Res. 2019;9: 1354-1366.

7. Novikova IV, Hennelly SP, Sanbonmatsu KY. Tackling structures of long noncoding RNAs. Int J Mol Sci. 2013;14: 23672-23684.
8. Schmitz SU, Grote P, Herrmann BG. Mechanisms of long noncoding RNA function in development and disease. Cell Mol Life Sci. 2016;73: 2491-2509.
9. Kazemzadeh M, Safaralizadeh R, Orang AV. LncRNAs: emerging players in gene regulation and disease pathogenesis. J Genet. 2015;94: 771-784.
10. Rinn JL, Kertesz M, Wang JK, et al. Functional demarcation of active and silent chromatin domains in human HOX loci by noncoding RNAs. Cell. 2007;129: 1311-1323.
11. Mondal T, Subhash S, Vaid R, et al. MEG3 long noncoding RNA regulates the TGF-beta pathway genes through formation of RNA-DNA triplex structures. Nat Commun. 2015;6: 7743.
12. Gibb EA, Brown CJ, Lam WL. The functional role of long non-coding RNA in human carcinomas. Mol Cancer. 2011;10: 38.
13. Yang F, Li J, Ge Q, et al. Non-coding RNAs: Emerging roles in the characterization of immune microenvironment and immunotherapy of prostate cancer. Biochem Pharmacol. 2023;214: 115669.
14. Ge WJ, Huang H, Wang T, et al. Long non-coding RNAs in hepatocellular carcinoma. Pathol Res Pract. 2023;248: 154604.
15. Mohammadpour S, Naderi Noukabadi F, Torshizi Esfahani A, et al. Non-coding RNAs in Precursor Lesions of Colorectal Cancer: Their Role in Cancer Initiation and Formation. Curr Mol Med. 2023.
16. Yin Q, Ma H, Bamunuarachchi G, Zheng X, Ma Y. Long Non-Coding RNAs, Cell Cycle, and Human Breast Cancer. Hum Gene Ther. 2023;34: 481-494.
17. Baba SK, Baba SK, Mir R, et al. Long non-coding RNAs modulate tumor microenvironment to promote metastasis: novel avenue for therapeutic intervention. Front Cell Dev Biol. 2023;11: 1164301.
18. Chao C, Tang R, Zhao J, Di D, Qian Y, Wang B. Oncogenic roles and related mechanisms of the long non-coding RNA MINCR in human cancers. Front Cell Dev Biol. 2023;11: 1087337.
19. Guzel E, Okyay TM, Yalcinkaya B, Karacaoglu S, Gocmen M, Akcakuyu MH. Tumor suppressor and oncogenic role of long non-coding RNAs in cancer. North Clin Istanb. 2020;7: 81-86.
20. Khan MR, Wellinger RJ, Laurent B. Exploring the Alternative Splicing of Long Noncoding RNAs. Trends Genet. 2021;37: 695-698.
21. Geisler S, Coller J. RNA in unexpected places: long non-coding RNA functions in diverse cellular contexts. Nat Rev Mol Cell Biol. 2013;14: 699-712.
22. Ulitsky I, Bartel DP. lincRNAs: genomics, evolution, and mechanisms. Cell. 2013;154: 26-46.
23. Batista PJ, Chang HY. Long noncoding RNAs: cellular address codes in development and disease. Cell. 2013;152: 1298-1307.
24. Cong S, Di X, Li R, et al. RBM10 regulates alternative splicing of lncRNA Neat1 to inhibit the invasion and metastasis of NSCLC. Cancer Cell Int. 2022;22: 338.
25. Saghaeian Jazi M, Samaei NM, Ghanei M, Shadmehr MB, Mowla SJ. Overexpression of the non-coding SOX2OT variants 4 and 7 in lung tumors suggests an oncogenic role in lung cancer. Tumour Biol. 2016;37: 10329-10338.
26. Chalfant CE, Rathman K, Pinkerman RL, et al. De novo ceramide regulates the alternative splicing of caspase 9 and Bcl-x in A549 lung adenocarcinoma cells. Dependence on protein phosphatase-1. J Biol Chem. 2002;277: 12587-12595.
27. Dobin A, Davis CA, Schlesinger F, et al. STAR: ultrafast universal RNA-seq aligner. Bioinformatics. 2013;29: 15-21.
28. Danecek P, Bonfield JK, Liddle J, et al. Twelve years of SAMtools and BCFtools. Gigascience. 2021;10.
29. Patro R, Duggal G, Love MI, Irizarry RA, Kingsford C. Salmon provides fast and bias-aware quantification of transcript expression. Nat Methods. 2017;14: 417-419.
30. Love MI, Huber W, Anders S. Moderated estimation of fold change and dispersion for RNA-seq data with DESeq2. Genome Biol. 2014;15: 550.
31. Wickham H. Advanced R. Second edition. ed. Boca Raton: CRC Press/Taylor & Francis Group, 2019.
32. Soneson C, Love MI, Robinson MD. Differential analyses for RNA-seq: transcript-level estimates improve gene-level inferences. F1000Res. 2015;4: 1521.
33. Durinck S, Spellman PT, Birney E, Huber W. Mapping identifiers for the integration of genomic datasets with the R/Bioconductor package biomaRt. Nat Protoc. 2009;4: 1184-1191.

34. Shen S, Park JW, Huang J, et al. MATS: a Bayesian framework for flexible detection of differential alternative splicing from RNA-Seq data. Nucleic Acids Res. 2012;40: e61.
35. Vu NT, Park MA, Shultz MD, Bulut GB, Ladd AC, Chalfant CE. Caspase-9b Interacts Directly with cIAP1 to Drive Agonist-Independent Activation of NF-kappaB and Lung Tumorigenesis. Cancer Res. 2016;76: 2977-2989.
36. Shultz JC, Goehe RW, Wijesinghe DS, et al. Alternative splicing of caspase 9 is modulated by the phosphoinositide 3-kinase/Akt pathway via phosphorylation of SRp30a. Cancer Res. 2010;70: 9185-9196.
37. Goehe RW, Shultz JC, Murudkar C, et al. hnRNP L regulates the tumorigenic capacity of lung cancer xenografts in mice via caspase-9 pre-mRNA processing. J Clin Invest. 2010;120: 3923-3939.
38. Vu NT, Park MA, Shultz JC, et al. hnRNP U enhances caspase-9 splicing and is modulated by AKT-dependent phosphorylation of hnRNP L. J Biol Chem. 2013;288: 8575-8584.
39. Shultz JC, Goehe RW, Murudkar CS, et al. SRSF1 regulates the alternative splicing of caspase 9 via a novel intronic splicing enhancer affecting the chemotherapeutic sensitivity of non-small cell lung cancer cells. Mol Cancer Res. 2011;9: 889-900.
40. Chalfant CE, Watson JE, Bisnauth LD, et al. Insulin regulates protein kinase CbetaII expression through enhanced exon inclusion in L6 skeletal muscle cells. A novel mechanism of insulin- and insulin-like growth factor-i-induced 5' splice site selection. J Biol Chem. 1998;273: 910-916.
41. Mietla JA, Wijesinghe DS, Hoeferlin LA, et al. Characterization of eicosanoid synthesis in a genetic ablation model of ceramide kinase. J Lipid Res. 2013;54: 1834-1847.
42. Simanshu DK, Kamlekar RK, Wijesinghe DS, et al. Non-vesicular trafficking by a ceramide-1-phosphate transfer protein regulates eicosanoids. Nature. 2013;500: 463-467.
43. Pettus BJ, Bielawska A, Subramanian P, et al. Ceramide 1-phosphate is a direct activator of cytosolic phospholipase A2. J Biol Chem. 2004;279: 11320-11326.
44. Lamour NF, Stahelin RV, Wijesinghe DS, et al. Ceramide kinase uses ceramide provided by ceramide transport protein: localization to organelles of eicosanoid synthesis. J Lipid Res. 2007;48: 1293-1304.
45. Lamour NF, Subramanian P, Wijesinghe DS, Stahelin RV, Bonventre JV, Chalfant CE. Ceramide 1-phosphate is required for the translocation of group IVA cytosolic phospholipase A2 and prostaglandin synthesis. J Biol Chem. 2009;284: 26897-26907.
46. Mishra SK, Gao YG, Deng Y, Chalfant CE, Hinchcliffe EH, Brown RE. CPTP: A sphingolipid transfer protein that regulates autophagy and inflammasome activation. Autophagy. 2018;14: 862-879.
47. Vu NT, Kim M, Stephenson DJ, MacKnight HP, Chalfant CE. Ceramide Kinase Inhibition Drives Ferroptosis and Sensitivity to Cisplatin in Mutant KRAS Lung Cancer by Dysregulating VDAC-Mediated Mitochondria Function. Mol Cancer Res. 2022;20: 1429-1442.
48. Kim M, Vu NT, Wang X, et al. Caspase 9b Drives Cellular Transformation, Lung Inflammation, and Lung Tumorigenesis. Mol Cancer Res. 2022;20: 1284-1294.
49. Massiello A, Chalfant CE. SRp30a (ASF/SF2) regulates the alternative splicing of caspase-9 pre-mRNA and is required for ceramide-responsiveness. J Lipid Res. 2006;47: 892-897.
50. Xie X, Piao L, Cavey GS, et al. Phosphorylation of Nanog is essential to regulate Bmi1 and promote tumorigenesis. Oncogene. 2014;33: 2040-2052.
51. Maus KD, Stephenson DJ, Ali AN, et al. Ceramide kinase regulates acute wound healing by suppressing 5-oxo-ETE biosynthesis and signaling via its receptor OXER1. J Lipid Res. 2022;63: 100187.
52. Maus KD, Stephenson DJ, Macknight HP, et al. Skewing cPLA(2)alpha activity toward oxoeicosanoid production promotes neutrophil N2 polarization, wound healing, and the response to sepsis. Sci Signal. 2023;16: eadd6527.
53. MacKnight HP, Stephenson DJ, Hoeferlin LA, et al. The interaction of ceramide 1-phosphate with group IVA cytosolic phospholipase A(2) coordinates acute wound healing and repair. Sci Signal. 2019;12.
54. Yamamoto M, Acevedo-Duncan M, Chalfant CE, Patel NA, Watson JE, Cooper DR. Acute glucose-induced downregulation of PKC-betaII accelerates cultured VSMC proliferation. Am J Physiol Cell Physiol. 2000;279: C587-595.
55. Patel NA, Chalfant CE, Yamamoto M, Watson JE, Eichler DC, Cooper DR. Acute hyperglycemia regulates transcription and posttranscriptional stability of PKCbetaII mRNA in vascular smooth muscle cells. FASEB J. 1999;13: 103-113.

569 56. Patel NA, Apostolatos HS, Mebert K, et al. Insulin regulates protein kinase CbetaII alternative
570 splicing in multiple target tissues: development of a hormonally responsive heterologous minigene. Mol
571 Endocrinol. 2004;18: 899-911.
572 57. Wijesinghe DS, Subramanian P, Lamour NF, et al. Chain length specificity for activation of
573 cPLA2alpha by C1P: use of the dodecane delivery system to determine lipid-specific effects. J Lipid Res.
574 2009;50: 1986-1995.
575 58. Subramanian P, Vora M, Gentile LB, Stahelin RV, Chalfant CE. Anionic lipids activate group IVA
576 cytosolic phospholipase A2 via distinct and separate mechanisms. J Lipid Res. 2007;48: 2701-2708.
577 59. Caslin HL, Abebayehu D, Abdul Qayum A, et al. Lactic Acid Inhibits Lipopolysaccharide-Induced
578 Mast Cell Function by Limiting Glycolysis and ATP Availability. J Immunol. 2019;203: 453-464.
579 60. Ghosh N, Patel N, Jiang K, et al. Ceramide-activated protein phosphatase involvement in insulin
580 resistance via Akt, serine/arginine-rich protein 40, and ribonucleic acid splicing in L6 skeletal muscle
581 cells. Endocrinology. 2007;148: 1359-1366.
582 61. Norton SK, Wijesinghe DS, Dellinger A, et al. Epoxyeicosatrienoic acids are involved in the C(70)
583 fullerene derivative-induced control of allergic asthma. J Allergy Clin Immunol. 2012;130: 761-769 e762.
584 62. Li R, Li Y, Kristiansen K, Wang J. SOAP: short oligonucleotide alignment program. Bioinformatics.
585 2008;24: 713-714.
586 63. Zhang B, Gunawardane L, Niazi F, Jahanbani F, Chen X, Valadkhan S. A novel RNA motif mediates
587 the strict nuclear localization of a long noncoding RNA. Mol Cell Biol. 2014;34: 2318-2329.
588 64. Zeng Y, Cullen BR. RNA interference in human cells is restricted to the cytoplasm. RNA. 2002;8:
589 855-860.
590 65. Faustino NA, Cooper TA. Pre-mRNA splicing and human disease. Genes Dev. 2003;17: 419-437.
591 66. Al-Khalaf HH, Aboussekhra A. p16(INK4A) positively regulates p21(WAF1) expression by
592 suppressing AUF1-dependent mRNA decay. PLoS One. 2013;8: e70133.
593 67. Tominaga M, Sueoka N, Irie K, et al. Detection and discrimination of preneoplastic and early stages
594 of lung adenocarcinoma using hnRNP B1 combined with the cell cycle-related markers p16, cyclin D1,
595 and Ki-67. Lung Cancer. 2003;40: 45-53.
596 68. Shultz JC, Chalfant CE. Caspase 9b: a new target for therapy in non-small-cell lung cancer. Expert
597 Rev Anticancer Ther. 2011;11: 499-502.
598 69. Lykke-Andersen S, Jensen TH. Nonsense-mediated mRNA decay: an intricate machinery that shapes
599 transcriptomes. Nat Rev Mol Cell Biol. 2015;16: 665-677.
600 70. Bridges MC, Daulagala AC, Kourtidis A. LNCcation: lncRNA localization and function. J Cell Biol.
601 2021;220.
602 71. Guo CJ, Xu G, Chen LL. Mechanisms of Long Noncoding RNA Nuclear Retention. Trends Biochem
603 Sci. 2020;45: 947-960.
604 72. Ariel F, Lucero L, Christ A, et al. R-Loop Mediated trans Action of the APOLO Long Noncoding
605 RNA. Mol Cell. 2020;77: 1055-1065 e1054.
606 73. Mishra K, Kanduri C. Understanding Long Noncoding RNA and Chromatin Interactions: What We
607 Know So Far. Noncoding RNA. 2019;5.
608 74. Kato M, Carninci P. Genome-Wide Technologies to Study RNA-Chromatin Interactions. Noncoding
609 RNA. 2020;6.
610 75. Benoit Bouvrette LP, Cody NAL, Bergalet J, et al. CeFra-seq reveals broad asymmetric mRNA and
611 noncoding RNA distribution profiles in Drosophila and human cells. RNA. 2018;24: 98-113.
612 76. Carlevaro-Fita J, Rahim A, Guigo R, Vardy LA, Johnson R. Cytoplasmic long noncoding RNAs are
613 frequently bound to and degraded at ribosomes in human cells. RNA. 2016;22: 867-882.
614 77. van Heesch S, van Iterson M, Jacobi J, et al. Extensive localization of long noncoding RNAs to the
615 cytosol and mono- and polyribosomal complexes. Genome Biol. 2014;15: R6.
616 78. Zhang M, Zeng J, Zhao Z, Liu Z. Loss of MiR-424-3p, not miR-424-5p, confers chemoresistance
617 through targeting YAP1 in non-small cell lung cancer. Mol Carcinog. 2017;56: 821-832.
618 79. Sun Y, Li L, Xing S, et al. miR-503-3p induces apoptosis of lung cancer cells by regulating p21 and
619 CDK4 expression. Cancer Biomark. 2017;20: 597-608.
620 80. Zhu Y, Zhu L, Wang X, Jin H. RNA-based therapeutics: an overview and prospectus. Cell Death Dis.
621 2022;13: 644.

622

623

624

625 **FIGURE LEGENDS**

626 **Figure 1. The association of CyKILR expression with an active, wild-type *STK11* and *CDKN2A* genes**
627 **in NSCLCs.** Total RNA was collected from the indicated NSCLC cell lines. Quantitative Real-Time PCR
628 (qRT-PCR) and deep RNA sequencing were conducted. The R program was used for analysis of deep RNA
629 sequencing data. Western immunoblotting were conducted on 12 NSCLC lines to assess the expression of
630 *CDKN2A* and *STK11* gene products with CyKILR expression. **A.** The mRNA level of CDKN2A across the
631 12 NSCLC lines normalized to GAPDH mRNA levels. **B.** Correlation plot of deep RNA sequencing data
632 displaying the relationship between *CDKN2A* gene status and the expression of the lncRNA, CyKILR. **C.**
633 CyKILR RNA levels by qRT-PCR across the 12 NSCLC lines normalized to GAPDH mRNA levels. Data
634 in Panels A and C are presented as mean (SD) ($n \geq 3$ replicates). **D.** Three-dimensional PCA plot
635 representing the variation of CDKN2A and CyKILR expression for the 12 NSCLC lines. **E.** The mRNA
636 level of the *STK11* gene product, LKB1, across the 12 NSCLC lines normalized to GAPDH mRNA levels.
637 Data in Panel E are presented as mean ± SD ($n \geq 3$ replicates). **F.** Correlation plot of deep RNA sequencing
638 data to an active, wild-type *STK11* gene displaying the relationship between *STK11* mRNA expression and
639 CyKILR expression. **G.** Relative protein levels of the indicated factors across a panel of 12 cell lines with
640 β-actin used for normalization. **H.** The protein levels of the *CDKN2A* gene products, p14 and p16, the
641 *STK11* gene product, LKB1, across the 12 NSCLC lines with β-actin used for normalization. Data in Panel
642 H are presented as mean ± SD ($n \geq 3$ replicates).

643 **Figure 2. CyKILR is characterized by two distinct isoform groups based on exon 3 inclusion/exclusion.**
644 Total RNA was collected from the indicated NSCLC cell lines. **A.** Short-read RNA sequencing was
645 conducted on these RNA samples. The CyKILR RNA splice variants were categorized into two distinct
646 groups based on the inclusion/exclusion of Exon 3 into the mature RNA transcript. **B.** The expression level
647 of CyKILR isoforms across the 12 cell lines. **C.** Relative RNA levels of CyKILRa (including Exon 3) and
648 CyKILRb (excluding Exon 3) variants across a panel of 12 NSCLC cell lines using RT-PCR. **D.** The RNA

649 expression levels of CyKILRa and CyKILRb are depicted by employing a customized quantitative primer
650 and probe strategy for the detection of CyKILRa and CyKILRb variants and normalized to GAPDH mRNA
651 levels. The data in Panel D are presented as mean (SD) ($n \geq 3$ replicates).

652 **Figure 3. CyKILRa and CyKILRb demonstrate differential cellular localization. A.** Sequence analysis
653 of exon 3 of CyKILR reveals a nuclear localization motif. **B.** Multiplex RT-PCR was used on subcellular
654 RNA samples obtained from the depicted cell lines. **C.** Quantitative RT-PCR (qRT-PCR) analysis was used
655 on subcellular RNA samples obtained from the depicted cell lines. The expression of nuclear and
656 cytoplasmic CyKILR RNA splicing variants is depicted for the individual cell lines. The data are presented
657 as boxplots ($n = 3$ replicates). Data in Panel C were analyzed by unpaired t-test with Welch's correction.

658 **Figure 4. CDKN2A and LKB1 concomitantly regulate the inclusion of exon 3 into CyKILR RNA.** The
659 depicted cell lines were transfected with scrambled control, CDKN2A, LKB1, or CDKN2A/LKB siRNAs.
660 After 48hrs, total protein and RNA were extracted. **A.** Protein levels of CDKN2A (p14 and p16) and LKB1
661 in samples subjected to single or double gene siRNA downregulation compared to scrambled siRNA
662 controls. **B.** The level of total CyKILR RNA was determined by qRT-PCR normalized to GAPDH in
663 samples subjected to single or double gene siRNA downregulation compared to scrambled siRNA controls.
664 **C.** The ratio of CyKILRb to CyKILRa RNA levels determined by qRT-PCR in samples subjected to single
665 or double gene siRNA downregulation compared to scrambled siRNA controls. **D.** The fold change of
666 proliferation analysis of CyKILRb silencing on double gene downregulation by siRNA (CDKN2A and
667 LKB1) compared to scrambled siRNA controls from day 5 to day 1 post-48hr silencing. Data were analyzed
668 by one-way ANOVA and presented as box plots ($n \geq 3$ replicates).

669 **Figure 5. Nuclear CyKILRa acts as a tumor suppressing factor.** The depicted cell lines were transfected
670 with scrambled control or CyKILRa ASO. After 48hrs, total RNA was extracted or in concomitant
671 experiments, the cells were assessed for the indicated biological mechanisms with the 48hr post-transfection
672 acting as the 0 time point. In addition, 48hr post-transfected H2009 and H1792 cells were subsequently
673 mixed with Matrigel in a 1:1 ratio and injected subcutaneously into the flanks of five-week-old female
674 NOD-SCID mice (1×10^6 cells per mouse per flank). The left flank received Control-treated cells, while
675 the right flank received knockdown cells. **A.** RNA levels of CyKILRa in the depicted cell lines post-ASO

treatment normalized to the mRNA levels of GAPDH. **B.** Proliferation of CyKILRa ASO-treated cells compared to scrambled control ASO-treated cells at the 48-hour time point. **C.** Migration of CyKILRa ASO-treated samples compared to scrambled control ASO-treated cells at the 24-hour time point. **D.** Colony formation of CyKILRa ASO-treated cells compared to scrambled control ASO-treated cells. **E.** Tumor volume of ASO-Con or ASO treated H2009 or H1792. The data are presented as box plots ($n \geq 3$ replicates), and statistical analysis was performed using the unpaired t-test with Welch's correction.

Figure 6. Cytoplasmic CyKILRb is a prosurvival factor. The depicted cell lines were transfected with scrambled control or CyKILRb siRNA. After 48hrs, total RNA was extracted or the cells were assessed for the indicated biological mechanisms with the 48hr post-transfection acting as the 0 time point. In addition, 48hr post-transfected H2009 and H1792 cells were subsequently mixed with Matrigel in a 1:1 ratio and injected subcutaneously into the flanks of five-week-old female NOD-SCID mice (1×10^6 cells per mouse per flank). The left flank received Scramble-treated cells, while the right flank received knockdown cells. **A.** RNA levels of CyKILRb siRNA-treated samples compared to scrambled siRNA control samples normalized to GAPDH mRNA. **B.** Proliferation of CyKILRb siRNA-treated cells compared to scrambled siRNA control cells at the 48-hour time point. **C.** Migration of CyKILRb siRNA-treated cells compared to scrambled siRNA control cells at the 24-hour time point. **D.** Colony formation of CyKILRb siRNA-treated cells compared to scrambled siRNA control cells. **E.** Tumor volume of siRNA-scramble control or si-RNA treated H2009 or H1792. The data are presented as box plots ($n \geq 3$ replicates), and statistical analysis was performed using the unpaired t-test with Welch's correction.

Figure 7. CyKILRa and CyKILRb apposingly regulate cell growth signaling pathways.

H2009 or H1792 cells were treated with either ASO-Con or ASO, and H1299 and H2009 cells were treated with either siRNA-Con or siRNA. Total RNA from these treatments underwent RNA sequencing. Following data filtering and clean read alignment, gene expression levels and differential expression gene analysis were conducted using RSEM (v1.2.28) and DESeq2. KEGG enrichment analysis of annotated differentially expressed genes was performed using R Phyper. The ASO-treated groups exhibited regulation of cell apoptosis and cell cycle pathways compared to the control-treated groups. While the siRNA-treated groups exhibited the regulation of microRNAs. **A.** Protein levels of key apoptosis markers were down-regulated

703 by ASO in all cell lines. **B.** Protein levels of key cell cycle markers were up-regulated by ASO in all cell
704 lines. **C.** Up-regulated microRNAs by CyKILRb knockdown in each cell line. **D.** Up-regulated microRNAs
705 by CyKILRb knockdown in both cell lines. **E.** The Venn diagram displays the upregulated miRNAs
706 resulting from CyKILRb knockdown in both H1299 and H2009 cell lines. **F.** RNA levels of miR-424-3P
707 and miR-503-3P in H1299 and H2009 cells treated with si-CyKILRb vs scramble control. **G.** Cell
708 proliferation assay comparing miR-424-3P and miR-503-3P mimic-treated H1299 and H2009 cells vs
709 scramble-treated cells 48 hours post-transfection. The data in Panels A, F, and G are presented as box plots
710 ($n \geq 3$ replicates), and statistical analysis was performed using the unpaired t-test with Welch's correction.
711

Figure 1

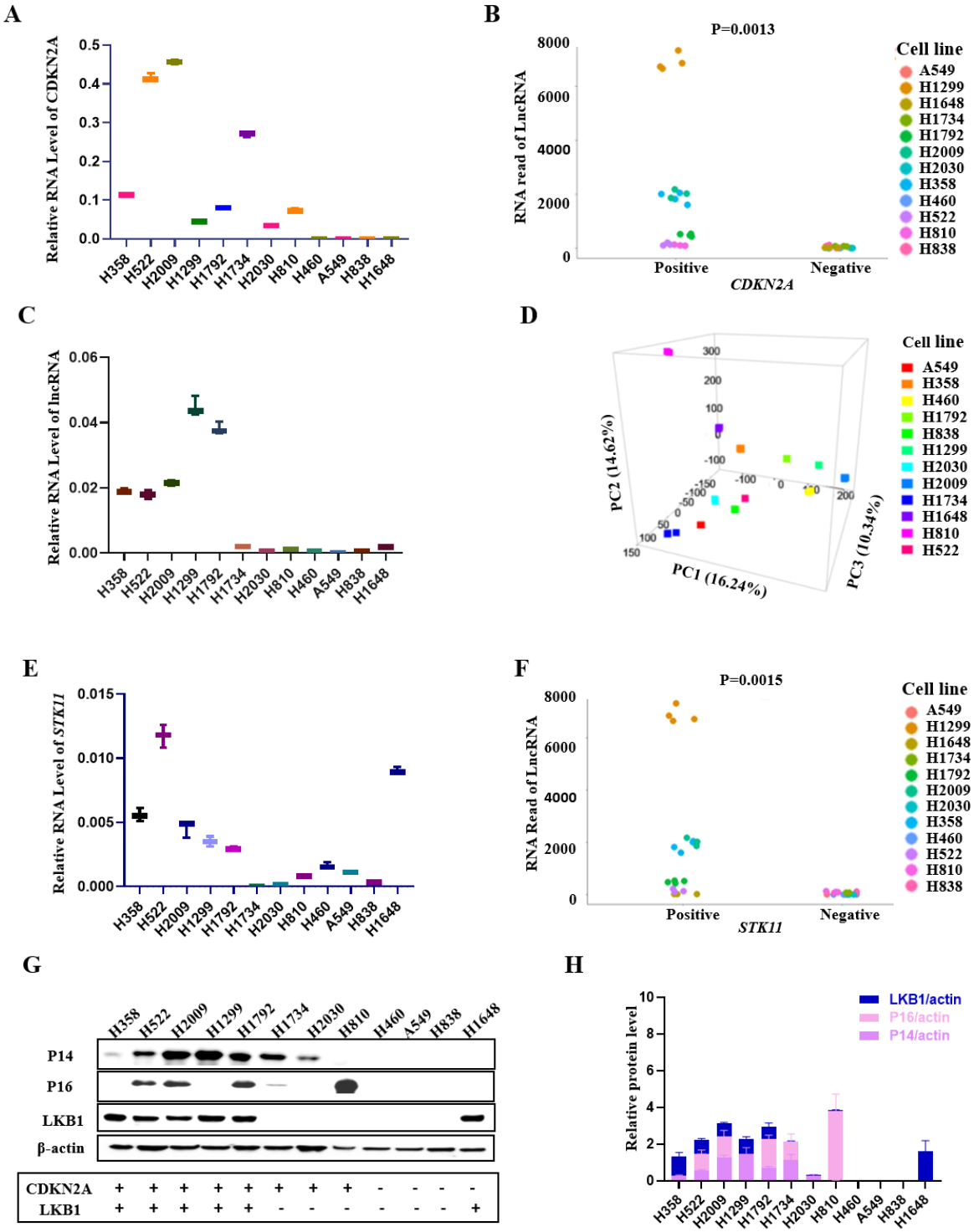
A
Relative RNA Level of CDKN2A
0.5
0.4
0.3
0.2
0.1
0.0
H358 H522 H2009 H1299 H1792 H1734 H2030 H810 H460 A549 H838 H1648
B
P=0.0013
RNA read of LncRNA
8000
6000
4000
2000
0
Positive
Negative
CDKN2A
Cell line
A549
H1299
H1648
H1734
H1792
H2009
H2030
H358
H460
H522
H810
H838
C
Relative RNA Level of lncRNA
0.06
0.04
0.02
0.00
H358 H522 H2009 H1299 H1792 H1734 H2030 H810 H460 A549 H838 H1648
D
PC2 (14.62%)
PC1 (16.24%)
PC3 (10.34%)
Cell line
A549
H358
H460
H1792
H838
H1299
H2030
H2009
H1734
H1648
H810
H522
E
Relative RNA Level of STK11
0.015
0.010
0.005
0.000
H358 H522 H2009 H1299 H1792 H1734 H2030 H810 H460 A549 H838 H1648
F
P=0.0015
RNA Read of LncRNA
8000
6000
4000
2000
0
Positive
Negative
STK11
Cell line
A549
H1299
H1648
H1734
H1792
H2009
H2030
H358
H460
H522
H810
H838
G
H358 H522 H2009 H1299 H1792 H1734 H2030 H810 H460 A549 H838 H1648
P14
P16
LKB1
β-actin
CDKN2A + + + + + + + + - - - -
LKB1 + + + + + - - - - - - +
H
Relative protein level
10
8
6
4
2
0
LKB1/actin
P16/actin
P14/actin
H358 H522 H2009 H1299 H1792 H1734 H2030 H810 H460 A549 H838 H1648

Figure 2

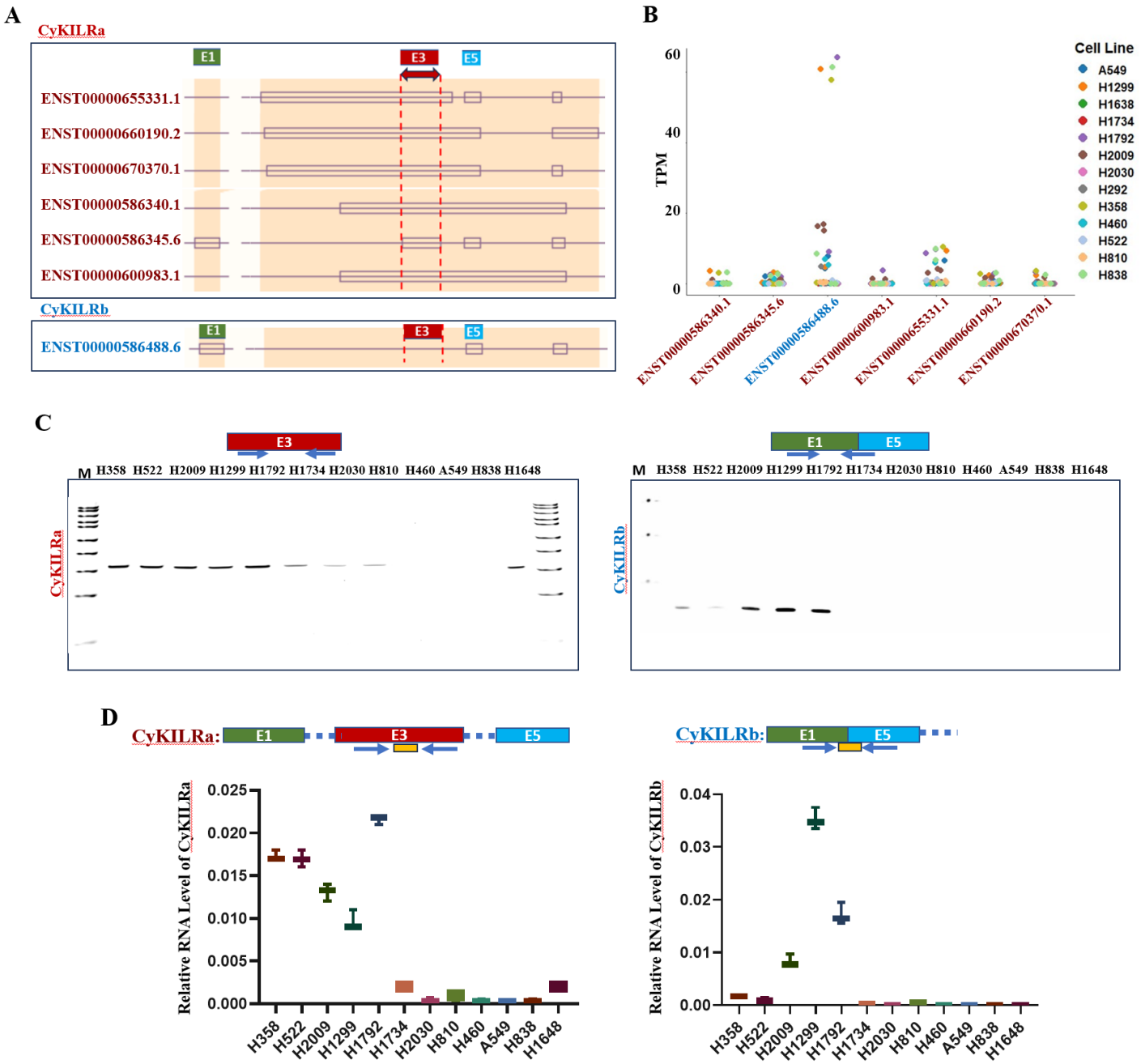
A
CyKILRa
E1
E3
E5
ENST00000655331.1
ENST00000660190.2
ENST00000670370.1
ENST00000586340.1
ENST00000586345.6
ENST00000600983.1
CyKILRb
ENST00000586488.6
B
TPM
Cell Line
A549
H1299
H1638
H1734
H1792
H2009
H2030
H292
H358
H460
H522
H810
H838
C
M H358 H522 H2009 H1299 H1792 H1734 H2030 H810 H460 A549 H838 H1648
D
CyKILRa:
CyKILRb:
Relative RNA Level of CyKILRa
Relative RNA Level of CyKILRb

Figure 3

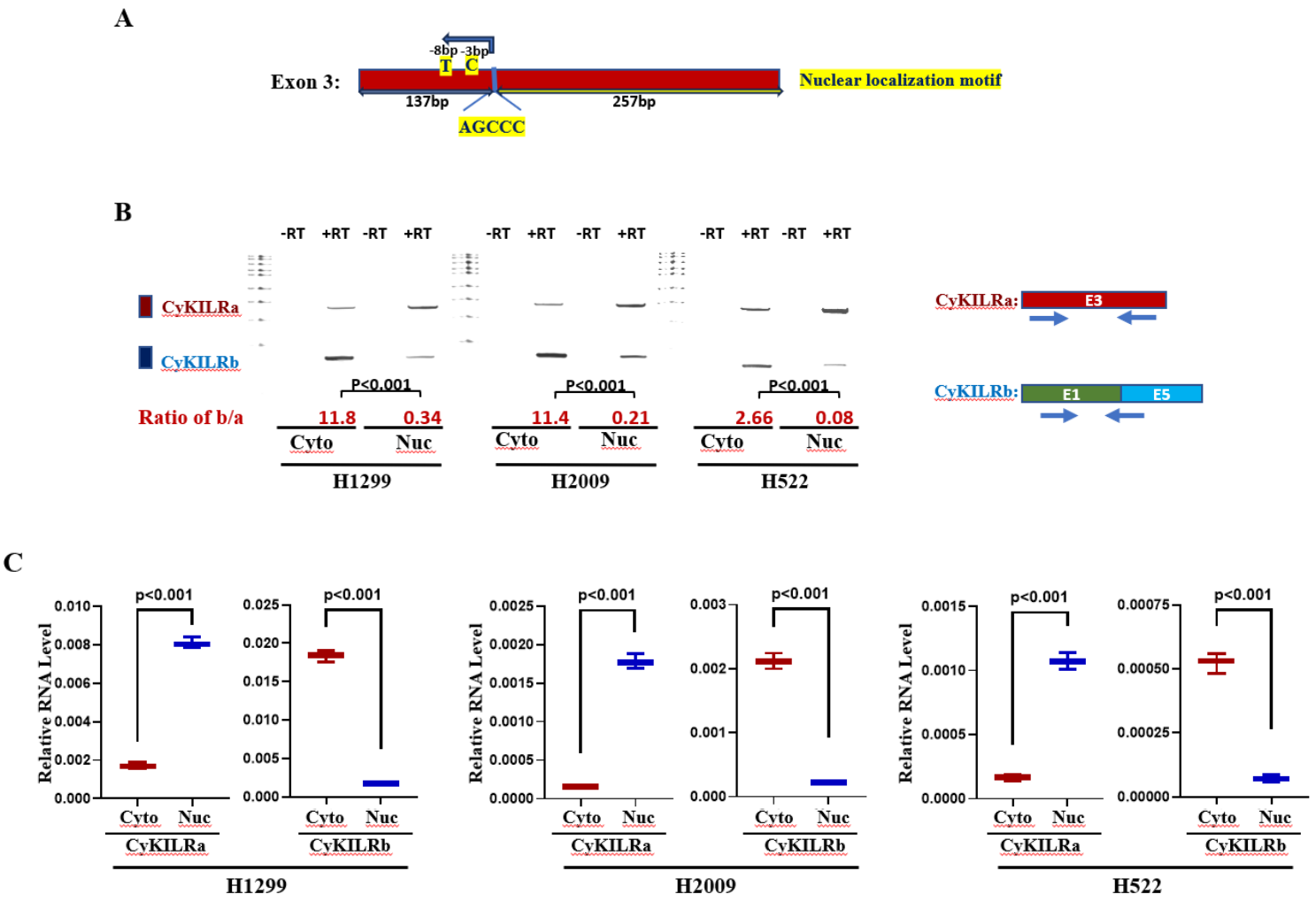
A
Exon 3:
-8bp -3bp
T C
137bp
257bp
AGCCC
Nuclear localization motif
B
-RT +RT -RT +RT
CyKILRa
CyKILRb
P<0.001
Ratio of b/a
11.8 0.34
11.4 0.21
2.66 0.08
Cyto Nuc
H1299
H2009
H522
CyKILRa: E3
CyKILRb: E1 E5
C
Relative RNA Level
p<0.001
Cyto Nuc
CyKILRa
CyKILRb
H1299
H2009
H522

Figure 4

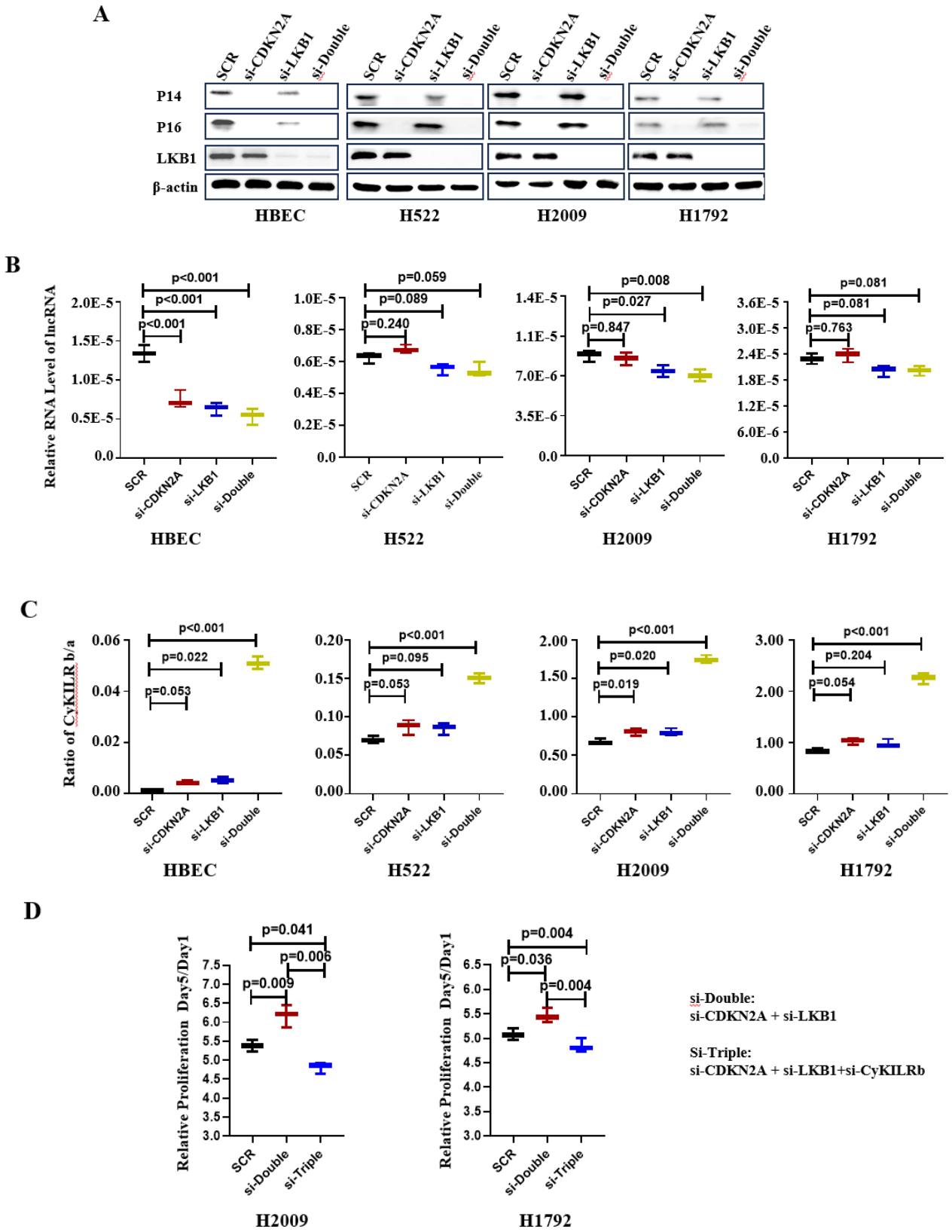
A
SCR
si-CDKN2A
si-LKB1
si-Double
P14
P16
LKB1
β-actin
HBEC
H522
H2009
H1792
B
Relative RNA Level of lncRNA
p<0.001
p<0.001
p<0.001
p=0.059
p=0.089
p=0.240
p=0.008
p=0.027
p=0.847
p=0.081
p=0.081
p=0.763
SCR
si-CDKN2A
si-LKB1
si-Double
HBEC
H522
H2009
H1792
C
Ratio of CyKILR b/a
p<0.001
p=0.022
p=0.053
p<0.001
p=0.095
p=0.053
p<0.001
p=0.020
p=0.019
p<0.001
p=0.204
p=0.054
SCR
si-CDKN2A
si-LKB1
si-Double
HBEC
H522
H2009
H1792
D
Relative Proliferation Day5/Day1
p=0.041
p=0.006
p=0.009
p=0.004
p=0.036
p=0.004
SCR
si-Double
si-Triple
H2009
H1792
si-Double:
si-CDKN2A + si-LKB1
Si-Triple:
si-CDKN2A + si-LKB1+si-CyKILRb

Figure 5

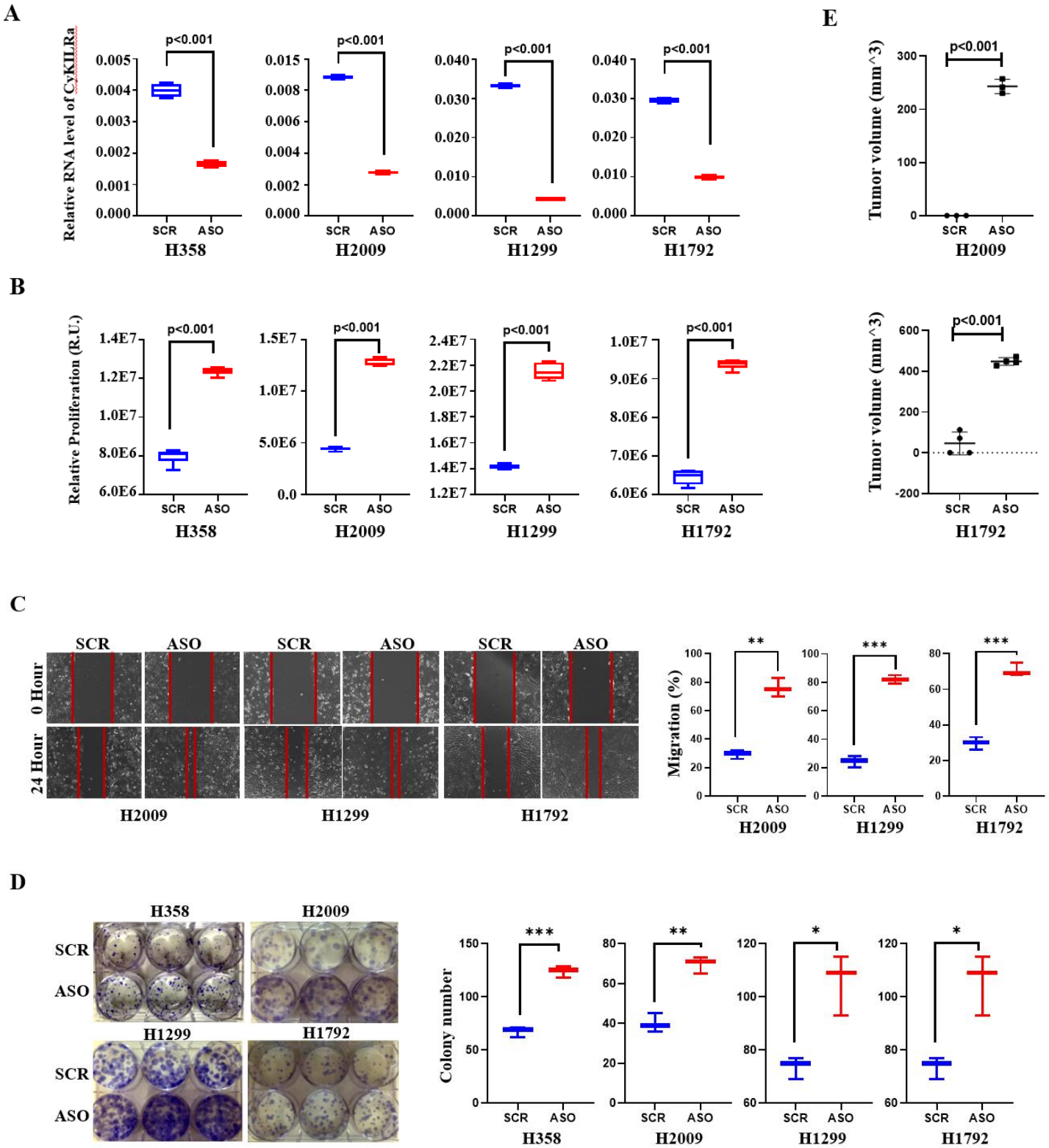
A
Relative RNA level of CyKILRa
p<0.001
SCR
ASO
H358
H2009
H1299
H1792
E
Tumor volume (mm^3)
H2009
B
Relative Proliferation (R.U.)
H1792
C
SCR
ASO
0 Hour
24 Hour
Migration (%)
**
***
D
Colony number
*

Figure 6

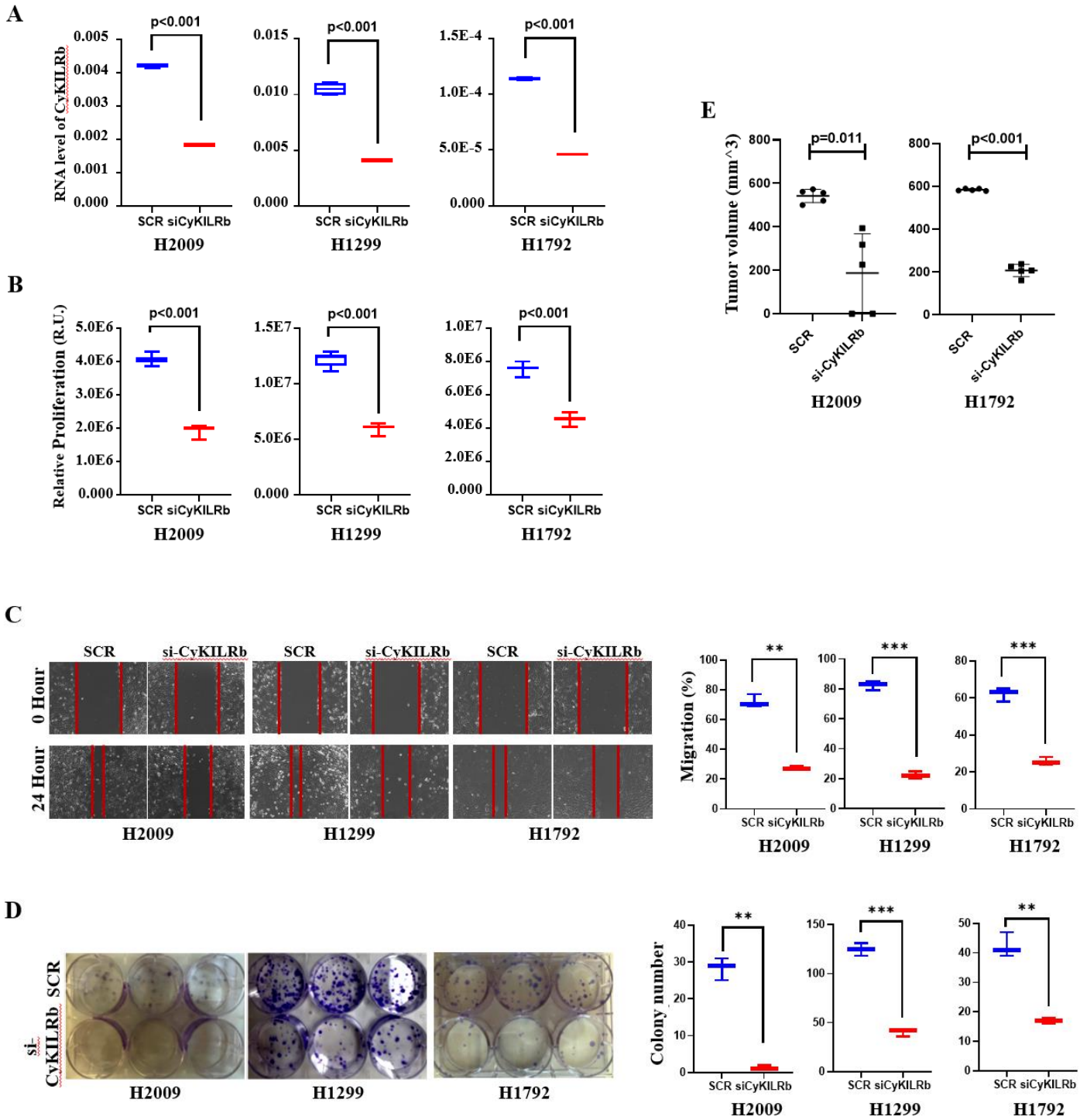
A
RNA level of CyKILRb
p<0.001
SCR siCyKILRb
H2009
H1299
H1792
B
Relative Proliferation (R.U.)
E
Tumor volume (mm^3)
p=0.011
SCR
si-CyKILRb
C
SCR
si-CyKILRb
0 Hour
24 Hour
Migration (%)
**
***
D
si-CyKILRb
Colony number

Figure 7

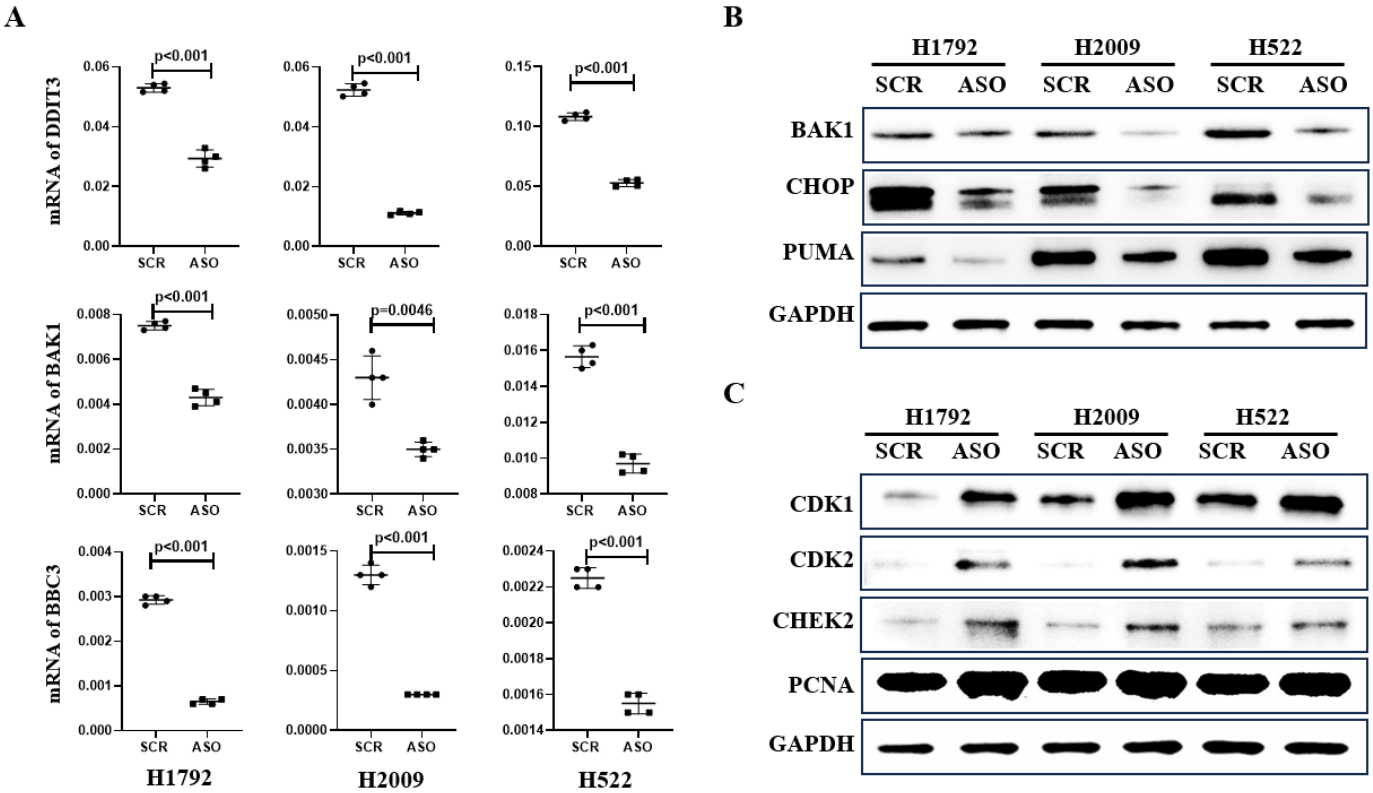
A
mRNA of DDIT3
mRNA of BAK1
mRNA of BBC3
p<0.001
p=0.0046
SCR
ASO
H1792
H2009
H522
B
H1792
H2009
H522
SCR
ASO
BAK1
CHOP
PUMA
GAPDH
C
CDK1
CDK2
CHEK2
PCNA
GAPDH

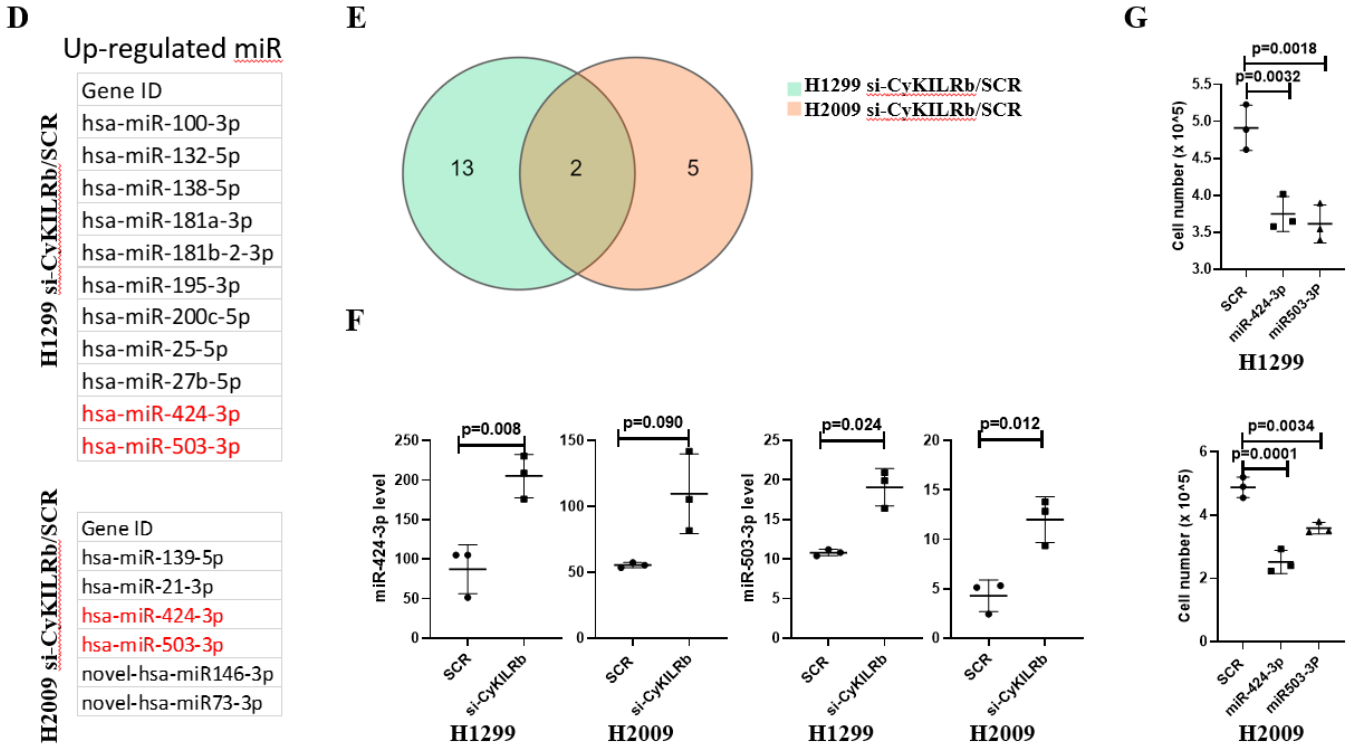
D
Up-regulated miR
H1299 si-CyKILRb/SCR
Gene ID
hsa-miR-100-3p
hsa-miR-132-5p
hsa-miR-138-5p
hsa-miR-181a-3p
hsa-miR-181b-2-3p
hsa-miR-195-3p
hsa-miR-200c-5p
hsa-miR-25-5p
hsa-miR-27b-5p
hsa-miR-424-3p
hsa-miR-503-3p
H2009 si-CyKILRb/SCR
Gene ID
hsa-miR-139-5p
hsa-miR-21-3p
hsa-miR-424-3p
hsa-miR-503-3p
novel-hsa-miR146-3p
novel-hsa-miR73-3p
E
13
2
5
H1299 si-CyKILRb/SCR
H2009 si-CyKILRb/SCR
F
miR-424-3p level
miR-503-3p level
p=0.008
p=0.090
p=0.024
p=0.012
SCR
si-CyKILRb
H1299
H2009
G
Cell number (x 10^5)
p=0.0018
p=0.0032
p=0.0034
p=0.0001
SCR
miR-424-3p
miR503-3P
H1299
H2009